

## Research Article

# Mathematical Model of Maximum Commutation Half Cycle for Thermal Countercurrent Oxidation of Low-Concentration Gas in Coal Mine Ventilation

Kuan Wu <sup>1,2</sup>, Shiliang Shi,<sup>1,2</sup> and Yong Chen <sup>1,2,3</sup>

<sup>1</sup>School of Resources, Environment and Safety Engineering, Hunan University of Science and Technology, Xiangtan, China

<sup>2</sup>Hunan University of Science and Technology Southern Coal Mine Gas and Roof Disaster Prevention and Control and Safety Production Key Experiment, Xiangtan, China

<sup>3</sup>China Coal Technology Engineering Group Chongqing Research Institute, Chongqing, China

Correspondence should be addressed to Kuan Wu; 170101020001@mail.hnust.edu.cn

Received 23 July 2021; Revised 12 September 2021; Accepted 14 September 2021; Published 13 October 2021

Academic Editor: Jianwei Cheng

Copyright © 2021 Kuan Wu et al. This is an open access article distributed under the Creative Commons Attribution License, which permits unrestricted use, distribution, and reproduction in any medium, provided the original work is properly cited.

The Fluent computational fluid dynamics software was used to study the relevant factors affecting the maximum commutation half cycle for thermal countercurrent oxidation of low-concentration gas in coal mine ventilation. Based on orthogonal experiments, the maximum commutation half cycle for thermal countercurrent oxidation of the exhaust gas in the coal mine ventilation under 25 working conditions with the combination of different methane concentrations, inlet speeds, porosities, and oxidation bed filling lengths is investigated. SPSS data processing software was used to perform regression analysis on the numerical simulation data, and a mathematical model for predicting the maximum commutation half cycle under the influence of four factors was obtained. Through experiments, the mathematical model of the maximum commutation half cycle by the numerical simulation was verified. After introducing the wall heat loss correction coefficient, the complete prediction model of the maximum commutation half cycle was obtained. Comparing the experimental test value with the calculated value using the corrected model, the relative error was not more than 3%. The complete mathematical model corrected can be applied to the design calculation of the maximum commutation half cycle for thermal countercurrent oxidation of low-concentration gas in actual coal mine ventilation.

## 1. Introduction

Coal is a fossil energy source which provides about 30% of the total energy consumption in the world [1–3]. Plenty of environmental problems and natural disasters may occur during coal mining, i.e., roof fall, gas, fire, and dust pollution [4–6]. Coal mine ventilation gas is the second most important greenhouse gas after carbon dioxide, and the effect of a unit mass of gas on the atmospheric greenhouse effect is 21 times that of the same mass of carbon dioxide. Coal mine ventilation is one of the main sources of industrial gas emissions. Reducing coal mine ventilation gas can reduce the greenhouse gas emissions. At the same time, the main component of the ventilation gas is methane, which is a high-quality and clean gas energy.

Therefore, reasonable recovery and utilization of coal mine ventilation gas have the dual significance of energy saving and environmental protection. The coal mine ventilation has the characteristics of large discharge amount, low gas concentration, and unstable concentration, making it difficult for coal mine ventilation gas to be burned directly without auxiliary fuel using traditional burners. At present, thermal countercurrent oxidation is one of the main technologies to achieve the reduction in low-concentration gas emission and rational utilization of coal mine ventilation. The key of this technology is to continuously change the flow direction of the gas fed into the reactor so that the ventilation gas can absorb heat and warm up in the heat accumulator to ensure the self-sustainability of the methane oxidation process [7–9].

So far, most studies on the thermal countercurrent oxidation of low-concentration gas in coal mine ventilation have focused on the temperature field of thermal countercurrent oxidation, methane conversion rate, and oxidation bed resistance and its influencing factors, while few studies on the maximum commutation half cycle for thermal counterflow oxidation of low-concentration gas in coal mine ventilation have been reported [10–15]. The authors of [16] reported the theoretical calculation formula of maximum half cycle of the reciprocating inert porous medium burner, which comprehensively considered the relationship of mutual restriction between the length of the burner, the gas supply parameters, the heating value of the gas, and the physical properties of the porous medium. However, the formula involved too many parameters. In addition to the burner length, methane concentration, inlet velocity, and porosity, the calculation also required adiabatic combustion temperature, the highest temperature of the combustion zone, effective thermal conductivity, etc. Thus, practical application has certain limitations, and the calculation formula did not consider the influence of wall heat loss. In this study, the orthogonal design and numerical simulation were combined to analyze the four influencing factors for the maximum commutation half cycle, and the mathematical model of the maximum commutation half cycle was obtained through regression analysis. Then, the obtained mathematical model was verified by the experiment of thermal countercurrent oxidation of low-concentration gas in coal mine ventilation, and the wall heat loss coefficient was introduced to correct the model. Finally, a complete prediction model of the maximum commutation half cycle was obtained, which can provide theoretical guidance for the design and operation of thermal countercurrent oxidation units for low-concentration gas in coal mine ventilation.

## 2. Principle of Thermal Countercurrent Oxidation of Coal Mine Ventilation Gas

As shown in Figure 1, when the device is started, the oxidation bed is preheated by the electric heating element, so that the central temperature reaches the ignition temperature (800°C). Coal mine ventilation gas flows into and through the oxidation bed in one direction, and the gas is heated by the heat exchange medium (honeycomb ceramic heat storage body). The temperature is continuously increased until the methane is oxidized. Then, the hot oxidized gas continues to move to the other end of the oxidation bed, transferring heat to the heat exchange medium and gradually cooling down. With the continuous entry of gas, the temperature on the inlet side of the oxidation bed gradually decreases and the temperature on the outlet side gradually increases. Before there is enough heat on the inlet side to heat the gas to the oxidation temperature, the commutation begins and the gas flow reverses. The key of the oxidation device is to continuously change the flow direction of the gas fed into the oxidation bed, so that the gas absorbs heat and warms up in the heat storage body, so as to ensure the self-sustainment of the oxidation process. At the same time, a heat exchanger is installed in the middle of the device to

recover part of the heat of the reaction, which is used to produce hot water or to generate power.

## 3. Numerical Simulation Scheme of Maximum Commutation Half Cycle

*3.1. Influencing Factors of Maximum Commutation Half Cycle.* The thermal countercurrent oxidation of low-concentration gas in coal mine ventilation needs to choose a suitable commutation half cycle. If the commutation half cycle is too small, it will cause a large amount of exhaust gas to be blown away without having time to oxidize during the commutation. In addition, the switching process causes instability of the air flow inside the device, which will inevitably cause adverse effects on the oxidation of methane. Therefore, the reversing time should be appropriately extended within the allowable range of the device to reduce the impact of the reversing process of the gas flow on the oxidation of methane. Moreover, extending the reversing time can increase the service life of the solenoid valve. However, an excessively large commutation half cycle will result in an excessively high outlet temperature, which is not conducive to heat accumulation. When the commutation half cycle is higher than the critical value, the highest temperature area of the oxidation bed is close to the outlet, the width of the high-temperature platform is too small, the exhaust gas cannot be completely oxidized, and the thermal countercurrent oxidation cannot be self-sustained. This critical commutation half cycle is regarded as the maximum commutation half cycle of thermal countercurrent oxidation.

The influencing factors of the maximum commutation half cycle for thermal countercurrent oxidation of low-concentration gas in coal mine ventilation include methane concentration, air inlet velocity, oxidation bed porosity, filling length, filling materials and physical properties of ventilation gas, and heat loss on the oxidation bed wall. The thermal countercurrent oxidation bed is usually filled with honeycomb ceramics and mostly made of cordierite and mullite. The physical properties of these two materials are relatively close. The methane concentration of coal mine ventilation gas is low, and the influence of methane concentration changes on its physical properties can be ignored, so the exhaust gas can be approximated as air. Therefore, the physical parameters of the filling material and the ventilation gas are fixed and can be considered as known quantities in the calculation. The wall heat loss is related to the thermal insulation performance of the oxidation bed device and the ambient temperature, and its influence on the maximum half cycle of the commutation is more complicated, so it is temporarily ignored in the numerical simulation analysis. Therefore, the factors affecting the maximum commutation half cycle of thermal countercurrent oxidation are simplified to four factors, i.e., methane concentration, inlet velocity, oxidation bed porosity, and filling length. This study first summarizes the mathematical model for the maximum commutation half cycle of thermal countercurrent oxidation under the action of 4 factors, then makes reasonable corrections to the mathematical model by considering the thermal insulation performance of the thermal

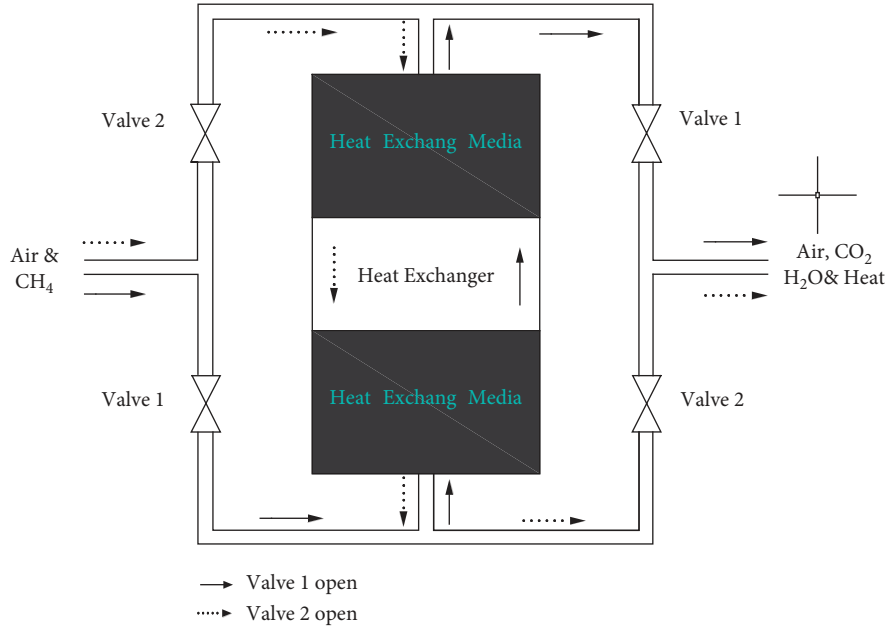


FIGURE 1: Schematic diagram of the thermal countercurrent oxidation device.

countercurrent oxidation system, and finally obtains a complete prediction mathematical model for the maximum commutation half cycle.

**3.2. Calculation Model.** In this paper, we simulated a self-designed thermal countercurrent oxidation device for coal mine ventilation, with the ventilation gas processing capability of  $500 \text{ m}^3/\text{h}$ . The thermal oxidation bed was a horizontal structure, and the air flowed left and right in the oxidation bed. The oxidation bed had a length of  $2.0 \text{ m}$ , a width of  $0.8 \text{ m}$ , and a height of  $0.8 \text{ m}$ , filling with several square honeycomb ceramics with the same specifications. Since the gas flow channels in the oxidation bed were evenly distributed and the equivalent diameter of the gas flow channels was much smaller than the size of the oxidation bed, the thermal oxidation bed can be considered as a uniform porous medium, and the equivalent continuous method can be used for simulation.

The simulation of the thermal countercurrent oxidation reaction of ventilation gas involves many aspects, including heat conduction, convection, radiation, and chemical

reaction. The detailed simulation of the process is computationally intensive. For simplicity, the following assumptions were made in the study [17–20]:

- (1) Honeycomb ceramics have good thermal conductivity and radiation ability, and the entire oxidation bed has a good thermal insulation performance. The temperature distribution in the oxidation bed is uniform. Thus, the simulation can be simplified to a one-dimensional problem.
- (2) Honeycomb ceramics have a large specific surface area, and the convective heat transfer coefficient between gas and solid is large enough. Therefore, there is a local thermal equilibrium between the gas and the solid, that is, their temperatures are equal at any point (single temperature model).
- (3) The porous medium is an optically thick medium.
- (4) The chemical reaction is simplified into a single-step overall reaction:

$$\text{state equation: } \rho_g = \frac{p}{RT}, \quad (1)$$

$$\text{continuity equation: } \varepsilon \frac{\partial \rho_g}{\partial t} + \frac{\partial}{\partial x} (\rho_g u) = 0, \quad (2)$$

$$\text{momentum equation: } \varepsilon \frac{\partial}{\partial t} (\rho_g u) + \frac{\partial}{\partial x} (\rho_g uu) = -\frac{\partial p}{\partial x} + \mu \frac{\partial^2 u}{\partial x^2} - C_x \frac{1}{2} \rho |u| u, \quad (3)$$

$$\text{energy equation: } (1 - \varepsilon) \frac{\partial}{\partial t} (\rho_s C_s T) + \varepsilon \frac{\partial}{\partial t} (\rho_g C_g T) + \frac{\partial}{\partial x} (\rho_g C_g T u) = \frac{\partial^2}{\partial x^2} (k_{\text{eff}} T) - \frac{\partial}{\partial x} \left( \sum_{i=1}^5 h_i J_i \right) + \varepsilon \Delta H \omega_{\text{CH}_4}, \quad (4)$$

$$\text{composition equation: } \varepsilon \frac{\partial}{\partial t} (\rho_g Y_i) + \frac{\partial}{\partial x} (\rho_g u Y_i) = -\frac{\partial}{\partial x} J_i + \varepsilon \omega_i. \quad (5)$$

The radiative transfer heat of porous media can be approximately described by the Rosseland model:

$$q_x(x) = -\frac{16}{3} \frac{\sigma T^3}{\alpha} \frac{dT}{dx}. \quad (6)$$

In the formulas, the subscript  $s$  represents the solid scalar and the subscript  $g$  represents the gas scalar. In the momentum equation (3),  $C_x$  is the internal resistance coefficient of porous media. In the energy equation (4), the effective thermal conductivity  $k_{\text{eff}} = k_e + k_r$ , is used as the thermal conductivity, where  $k_r = (16/3)(\sigma T^3/\alpha)$ , in which  $\alpha$  is the attenuation coefficient ( $\text{m}^{-1}$ ) and  $\sigma$  is the Stefan–Boltzmann constant,  $5.672 \times 10^{-8} \text{ W}/(\text{m} \cdot \text{K})$ ;  $k_e$  is the equivalent thermal conductivity of gas and solid, and its calculation method can be found in the literature [11].  $\omega_i$  is the mass generation rate of the  $i$ th substance,  $h_i$  is the specific enthalpy of the  $i$ th substance,  $H$  is the heat of reaction,  $Y_i$  is the mass fraction of the  $i$ th substance, and  $J_i$  is the diffusion flux of component  $i$ ,  $J_i = \rho_g D_i \nabla Y_i$ .

### 3.3. Single Value Condition

**3.3.1. Boundary Conditions.** Considering the ventilation gas mixture as an ideal gas, the inlet boundary condition uses the velocity inlet boundary condition to describe the ventilation gas flow at the inlet of the oxidation bed and the mass fraction of each component in the ventilation gas. The flow direction is perpendicular to the inlet plane, and the air temperature is set to 300 K. The outlet of the oxidation bed uses the pressure outlet boundary. Assuming that the flow is fully developed, the first derivative of the outlet boundary in the normal direction is zero. It is also necessary to define the “reflux” condition on the pressure outlet boundary, which is a practical boundary condition when fluid enters the calculation domain from the outside and a backflow occurs on the pressure outlet boundary. The strong oxidation reaction in the thermal oxidation bed may cause the backflow phenomenon at the outlet. The composition of the backflow gas is air, so the mass fraction of methane is 0 and the mass fraction of oxygen is 0.23.

**3.3.2. Commutation Conditions.** The time that the ventilation gas continuously flows in one direction in the oxidation bed is called a half commutation cycle, and the commutation action is completed instantaneously without time. The flow state, temperature, and physical property parameters of the gas as well as the physical property parameters of the ceramic honeycomb body did not change before and after the commutation moment.

The ventilation gas enters the oxidation bed from one end of the oxidation bed and changes direction after lasting for a half cycle. The original pressure outlet becomes a velocity inlet. The inlet velocity and direction and gas composition are the same as the previous half cycle. The original velocity inlet becomes pressure outlet, the export parameter setting is the same as the first half cycle. In this way, a forward–reverse continuous flow time of the mixed gas in the oxidation bed constitutes a commutation cycle, and this cycle is carried out until it enters a stable state. In Fluent, the periodic switching of boundary conditions was realized by running the journal file, and the cyclic calculation was completed.

**3.3.3. Initial Conditions.** Prior to system operation, the oxidation bed needs to be preheated to reach the temperature required for the ventilation gas oxidation, so as to enable the device to operate self-sustainably. Studies have shown that, after the oxidation bed enters stable operation, the operating state has nothing to do with the start-up process. Therefore, in the numerical simulation in this study, the influence of the start-up process of the oxidation bed was not considered, and only the influence of physical parameters and operating parameters on the performance of the oxidation bed during the operation was investigated. Meanwhile, the initial temperature of the porous medium was set to the temperature distribution function of the oxidation bed at the end of the start-up process, and the UDF program was imported into Fluent to realize the initialization of the temperature field of the oxidation bed. The initial concentration and temperature were the same as the parameters of the inlet ventilation gas.

**3.4. Numerical Simulation Solutions.** This study combined orthogonal design and numerical simulation to investigate the maximum commutation half cycle. Orthogonal experimental design is an experimental design method that studies multiple factors and multiple levels. It can achieve results equivalent to a large number of comprehensive experiments with the minimal number of tests. Before the orthogonal test, the test plan was first determined through the orthogonal table. The influencing factors of the maximum commutation half cycle for the thermal countercurrent oxidation of low-concentration gas in coal mine ventilation include methane concentration, air inlet velocity, oxidation bed porosity, filling length, filling materials, physical properties of ventilation gas, and heat loss on the oxidation bed wall. The thermal countercurrent oxidation bed is usually filled with honeycomb ceramics, mostly made of cordierite and mullite. These two materials have relatively

close physical properties. The methane concentration of coal mine ventilation gas is low, and the influence of methane concentration changes on its physical properties can be ignored, so the exhaust gas can be approximated as air. The physical parameters of the filling material and the ventilation gas were fixed; thus, they were considered as quantities in the calculation. The wall heat loss is related to the thermal insulation performance of the oxidation bed device and the ambient temperature, and its influence on the maximum half cycle of the commutation is more complicated. Therefore, the wall heat loss was temporarily ignored in the numerical simulation analysis.

Therefore, the four influencing factors of the maximum commutation half cycle ( $T$ ), i.e., methane concentration ( $c$ ), inlet velocity ( $v$ ), oxidation bed porosity ( $\varepsilon$ ), and filling length ( $L$ ), were used as independent variables for orthogonal design. According to the preliminary site inspection and actual measurement, comprehensively considering the oxidation effect and application conditions of the exhaust gas, we determined the level range corresponding to the four factors and designed the orthogonal test table. Meanwhile, in order to highlight the uniformity of the selected values and the disparity of results, the experimental program was designed in an equally spaced manner, with 5 levels for each factor. Thus, the "4 factors, 5 levels" orthogonal experimental design method was adopted in the study. Based on the above parameters and spatial location determination principles, the orthogonal test table was designed. The factors and levels are shown in Table 1.

#### 4. Simulation Results and Analysis

In order to investigate the influencing factors of the maximum commutation half cycle for the thermal countercurrent oxidation of low-concentration gas in coal mine ventilation, a total of 25 working conditions with the combination of different methane concentrations, inlet velocities, porosities, and oxidation bed filling lengths through orthogonal tables were used to perform numerical simulation. The simulation results are shown in Table 2.

According to the theory of orthogonal test, each factor was averaged at the same level to obtain the comprehensive average value of each factor at the same level. Then, the difference between the maximum value and the minimum value among the average values of different levels of each factor was calculated to obtain the range ( $r$ ) of each influencing factor. The range value can reflect the significance of the influence of the factor on the result. The larger the range value, the greater the difference in the level of the factor and the more important the factor. Through the range analysis, the influences of each factor on the different maximum commutation half cycle of thermal countercurrent oxidation can be derived. Figure 2 shows the fitting curves and ranges of the comprehensive average of the 4 factors.

It can be found from Figure 2 that the range between the maximum and minimum values of the inlet velocity is the largest among the four factors, indicating that the inlet velocity is the most important factor affecting the maximum commutation half cycle for the thermal countercurrent oxidation of

TABLE 1: Influencing factors and levels of the orthogonal test.

| Group number | $c$ (%) | $v$ (m/s) | $L$ (m) | $\varepsilon$ |
|--------------|---------|-----------|---------|---------------|
| 1            | 0.25    | 0.10      | 0.6     | 0.65          |
| 2            | 0.50    | 0.15      | 0.8     | 0.70          |
| 3            | 0.75    | 0.20      | 1.0     | 0.75          |
| 4            | 1.00    | 0.25      | 1.2     | 0.80          |
| 5            | 1.25    | 0.30      | 1.4     | 0.85          |

TABLE 2: Numerical simulation results.

| Test number | $c$ (%) | $v$ (m/s) | $L$ (m) | $\varepsilon$ | $T$ (min) |
|-------------|---------|-----------|---------|---------------|-----------|
| 1           | 0.25    | 0.10      | 0.6     | 0.65          | 20.63     |
| 2           | 0.25    | 0.15      | 0.8     | 0.70          | 14.32     |
| 3           | 0.25    | 0.20      | 1.0     | 0.75          | 10.28     |
| 4           | 0.25    | 0.25      | 1.2     | 0.80          | 7.23      |
| 5           | 0.25    | 0.30      | 1.4     | 0.85          | 4.73      |
| 6           | 0.50    | 0.10      | 0.8     | 0.75          | 28.51     |
| 7           | 0.50    | 0.15      | 1.0     | 0.80          | 17.09     |
| 8           | 0.50    | 0.20      | 1.2     | 0.85          | 10.36     |
| 9           | 0.50    | 0.25      | 1.4     | 0.65          | 25.98     |
| 10          | 0.50    | 0.30      | 0.6     | 0.70          | 7.20      |
| 11          | 0.75    | 0.10      | 1.0     | 0.85          | 25.05     |
| 12          | 0.75    | 0.15      | 1.2     | 0.65          | 51.54     |
| 13          | 0.75    | 0.20      | 1.4     | 0.70          | 36.02     |
| 14          | 0.75    | 0.25      | 0.6     | 0.75          | 9.30      |
| 15          | 0.75    | 0.30      | 0.8     | 0.80          | 7.68      |
| 16          | 1.00    | 0.10      | 1.2     | 0.70          | 81.71     |
| 17          | 1.00    | 0.15      | 1.4     | 0.75          | 48.31     |
| 18          | 1.00    | 0.20      | 0.6     | 0.80          | 11.11     |
| 19          | 1.00    | 0.25      | 0.8     | 0.85          | 8.07      |
| 20          | 1.00    | 0.30      | 1.0     | 0.65          | 22.95     |
| 21          | 1.25    | 0.10      | 1.4     | 0.80          | 67.89     |
| 22          | 1.25    | 0.15      | 0.6     | 0.85          | 12.68     |
| 23          | 1.25    | 0.20      | 0.8     | 0.65          | 33.63     |
| 24          | 1.25    | 0.25      | 1.0     | 0.70          | 27.12     |
| 25          | 1.25    | 0.30      | 1.2     | 0.75          | 21.25     |

low-concentration gas in coal mine ventilation. The influence of the 4 factors on the maximum commutation half cycle of thermal countercurrent oxidation can be ordered from high to low as  $v > L > c > \varepsilon$ . From Figure 2(a), as methane concentration increases, the maximum commutation half cycle gradually increases, which is mainly because the increase of the methane concentration in the exhaust gas leads to the increase of the heat entering the oxidation bed. Figure 2(b) shows that, as the inlet velocity increases, the maximum commutation half cycle gradually decreases. This is mainly because the increased inlet velocity causes the increase in the outlet heat loss, thereby reducing the commutation time. Figures 2(c) and 2(d) show that the maximum commutation half cycle increases with the increase of the oxidation bed filling length and decreases with the increase of the porosity of the oxidation bed. The reason is that when the porosity of the oxidation bed is larger, the solid area is smaller and the heat storage capacity of the oxidation bed is worse; thus, the fresh exhaust gas cools the inlet end more vigorously and the reversing time is shortened. As the filling length of the oxidation bed increases, the length of the oxidation bed preheating section is also correspondingly increased, and the heat stored in the oxidation bed increases, thereby prolonging the reversing time.

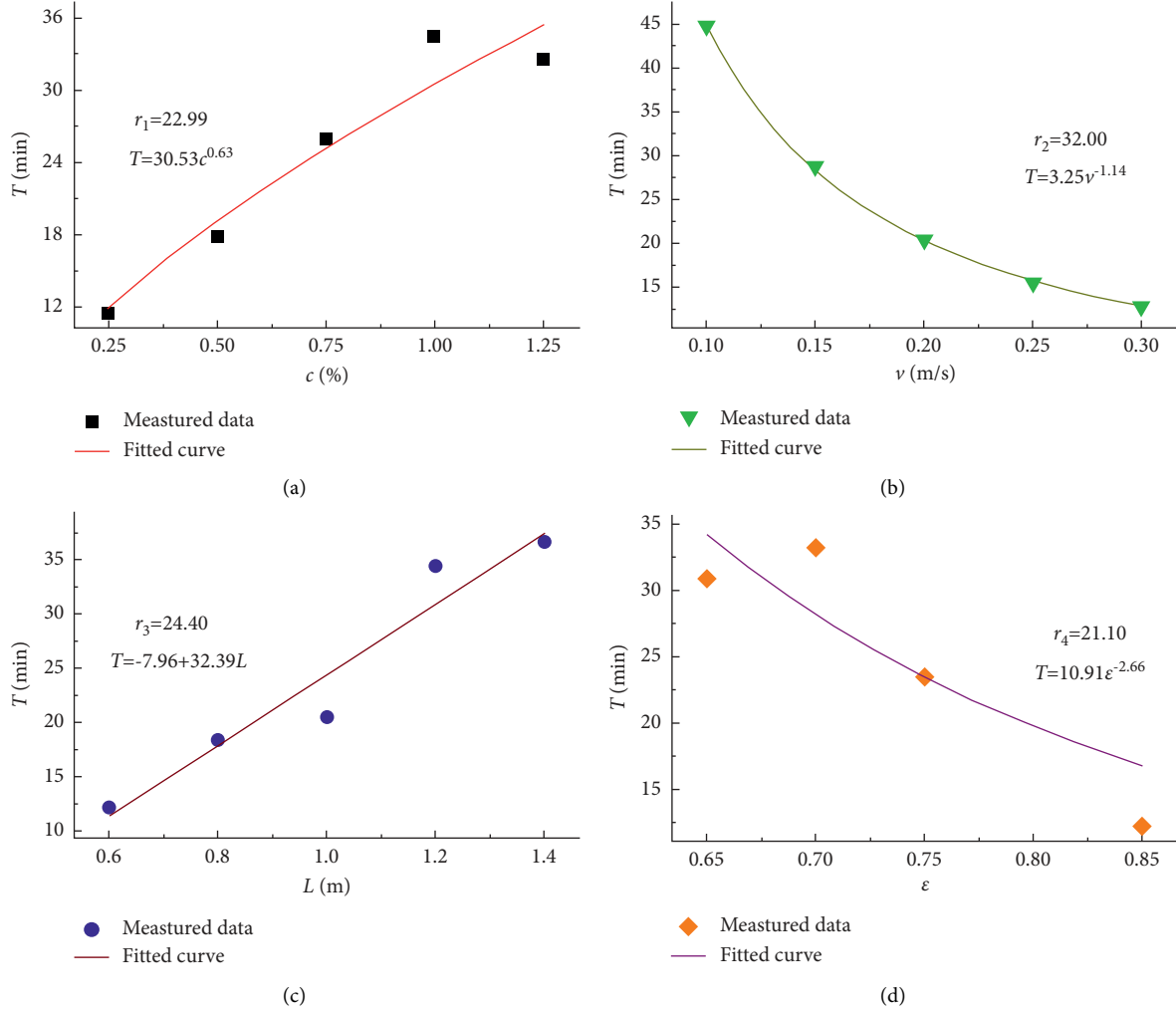


FIGURE 2: Comprehensive average values and ranges of 4 factors.

## 5. Establishment and Correction of Mathematical Model

**5.1. Multiple Nonlinear Regression Equation.** According to the fitting curve of the comprehensive average of the four factors, the influence of the filling length of the oxidation bed on the maximum commutation half cycle is linear, while the influence of the exhaust gas inlet velocity, methane concentration, and porosity on the maximum commutation half cycle is nonlinear, which can be more suitably described by the power function. On the basis of the above numerical simulation analysis, combined with the theoretical calculation formula of the maximum half cycle of the reciprocating inert porous medium burner in the literature [9], the relationship between the maximum half cycle and the influencing factors can be determined by the following objective function:

$$T = a_1 L (1 - \varepsilon)^{a_2} v^{a_3} c^{a_4}, \quad (7)$$

where  $a_1$  is the coefficient to be solved;  $a_2$ ,  $a_3$ , and  $a_4$  are the indexes to be solved;  $T$  is the maximum commutation half cycle, min;  $L$  is the length of the oxidation bed, m;  $\varepsilon$  is the

porosity of the oxidation bed;  $c$  is the methane concentration of the ventilation gas, %; and  $v$  is the air inlet velocity, m/s.

According to the 25 sets of sample data in Table 2, we selected nonlinear regression in SPSS, input the regression model into the model expression, and set the initial value and constraints. Then, the coefficient to be solved,  $a_1$ , and the indexes to be solved,  $a_2$ ,  $a_3$ , and  $a_4$ , were calculated, and the calculation equation of the maximum commutation half cycle was obtained as follows:

$$T = 23.433L(1 - \varepsilon)^{1.189} v^{-1.088} c^{0.654}. \quad (8)$$

From the calculated statistical report, it can be found that the relative deviation between the numerical simulation data and the formula calculation data did not exceed 10%, and  $R^2$  was 0.997. It can also be seen from the comparison result in Figure 3 that there is a good agreement between the formula calculation results and the numerical simulation results.

**5.2. Verification and Revision of Mathematical Model.** In order to experimentally verify the prediction mathematical model of the maximum commutation half cycle obtained by

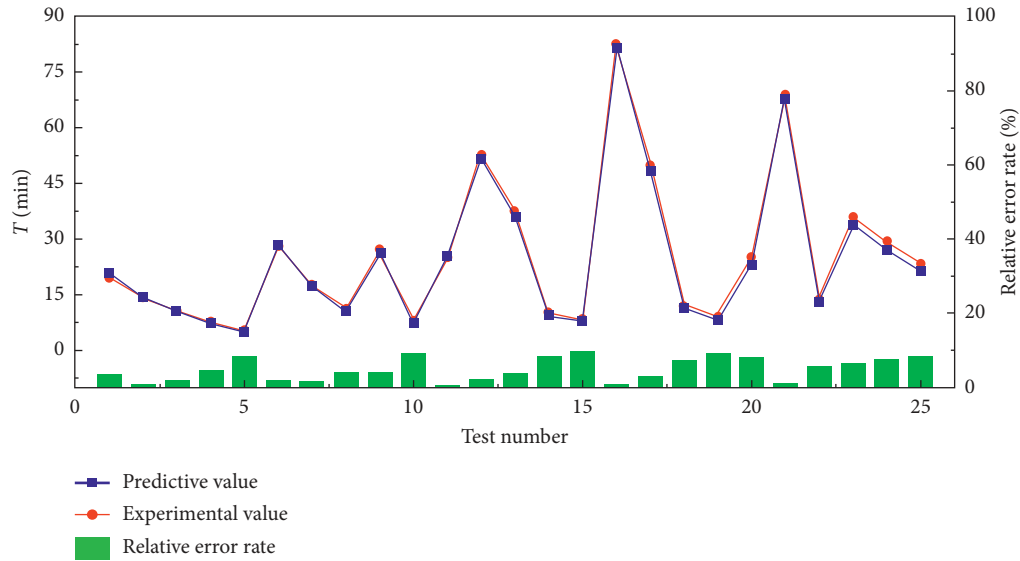


FIGURE 3: Comparison of numerical simulation values and formula calculation values.

numerical simulation regression analysis, an experimental system for thermal countercurrent oxidation of low-concentration gas in coal mine ventilation was established. The experimental system consisted of five parts: gas supply system, temperature acquisition system, water cooling system, gas composition analysis system, and the device body. The entire experimental system is shown in Figure 4. The compressed air from the air compressor was mixed with the methane gas from the methane cylinder at a certain volume ratio through the regulator valve and pressure reducing valve to obtain the simulated ventilation gas. The time relay and the solenoid valve cooperated with each other to make the simulated gas enter and discharge alternately from both ends of the oxidation bed of the device body. Fifteen thermocouples were evenly arranged in the direction of the central axis of the oxidation bed in the device body to monitor the temperature of the oxidation bed along the axis and at the inlet and outlet. The temperature data was collected through the acquisition card and displayed and stored in the computer in real time. The preheating temperature and heating power of the electric heater were controlled by using the temperature controller. In order to protect the solenoid valve, water coolers were provided at both ends of the device body to cool the outlet high-temperature exhaust gas. The gas chromatograph was used to detect the methane concentration in the intake and exhaust gas online.

After connecting the experimental system and ensuring the air tightness of the experimental instruments, equipment, and connecting parts, the experiment can begin. The experimental steps are as follows:

- (1) Turn on the main power switch of the device and power up the system. Then, start the air compressor to make the gas enter the air tank for storage first, and the air compressor is kept in an open position.
- (2) Turn on the time relay, set the commutation time, and the commutation control system will start to work. Turn on the computer connected to the data

acquisition card and open the data acquisition operating system on the computer. Set the channels and parameters that need to be collected and display the indicated values of each parameter in real time.

- (3) Open the methane cylinder container and adjust the outlet pressure to 0.2 MPa through the pressure reducing valve.
- (4) Subsequently, open the valves for air and methane and adjust them to their preset flow rates, and then make corresponding fine adjustments to make the displayed value consistent with the preset value.
- (5) Run the system under a fixed commutation cycle. When the temperature difference between the current circle and the next cycle does not exceed  $0.1^{\circ}\text{C}$ , the system can be considered in the stable operation. After the measured parameters have reached the required values, the system is considered to be successfully started. Then, we can start the formal experiments.
- (6) Adjust the parameters of each operating condition according to the experimental conditions. After the adjustment, the system is allowed to run for a certain period of time. Then, determine whether the system is in a stable state or not by observing the difference in temperature between the measured points of the oxidation bed in two consecutive cycles. After the condition stabilizes, the data can be collected and recorded. In the next working condition, repeat the above process to obtain the corresponding experimental results.
- (7) At the end of the experiment, first turn off the methane gas source, close the methane pressure reducing valve, stop data collection, save the experimental data, and then turn off the computer.
- (8) Turn off the flow meter, and then turn off the air source and the periodic commutation control



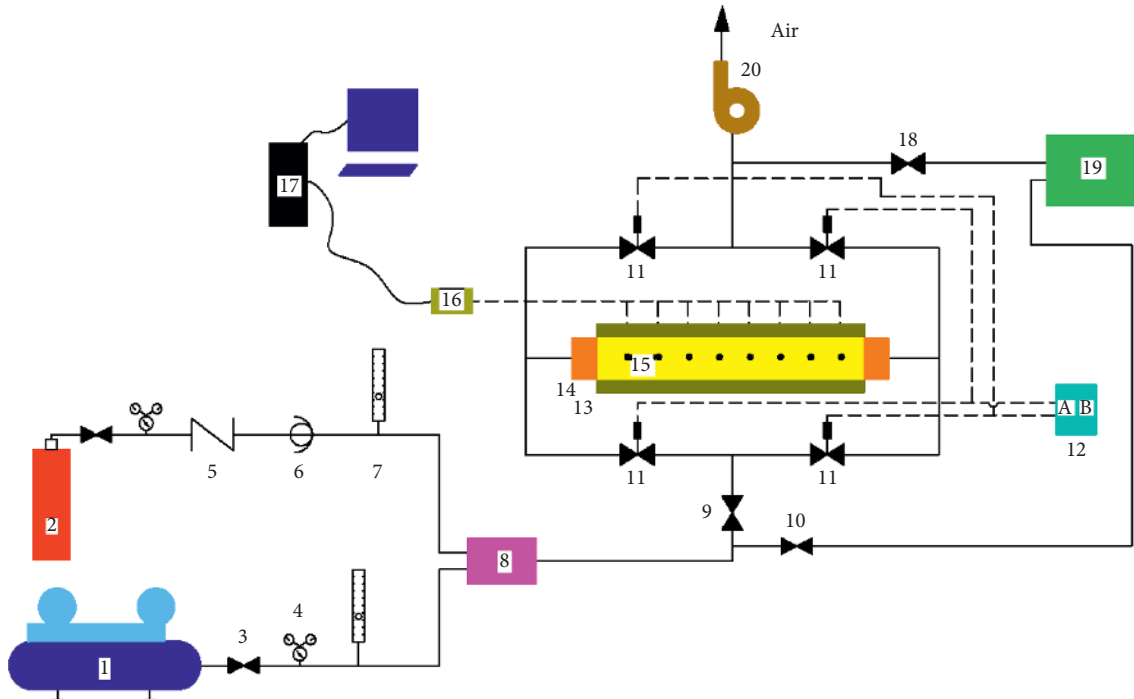


FIGURE 4: Experimental system for thermal countercurrent oxidation of low-concentration gas in coal mine ventilation (1: air compressor; 2: methane cylinder; 3: regulating valve; 4: pressure reducing valve; 5: one-way valve; 6: flame arrester; 7: rotor flow meter; 8: mixer; 9: intake main valve; 10: intake sampling valve (usually closed); 11: solenoid valve; 12: time relay; 13: device main body; 14: cooler; 15: thermocouple; 16: collection card; 17: computer; 18: exhaust gas sampling valve (usually closed); 19: gas chromatograph; 20: draft fan).

system. Turn off the power of the console, properly store the experimental instruments, and end the experiment.

(9) For the next experiment, repeat the above operation.

Four specifications of honeycomb ceramics were used in the experiment, two of which had the porosities of 0.56 and 0.70, with a square channel shape; and the other two had the porosities of 0.36 and 0.4, with a circular channel shape. The channel was square. The filling length of the oxidation bed was determined by the filling quantity of the honeycomb ceramics. The experiment only investigated the two cases with filling lengths of 0.8 m and 1.2 m. The methane concentration of the simulated gas was adjusted by controlling the two gas flow rates, and the inlet velocity was controlled by the intake valve. The commutation half cycle of the thermal countercurrent oxidation was manually set by the time relay. By changing the methane concentration, inlet velocity, porosity, and filling length, the measured values of the maximum commutation half cycle under the five combined working conditions were obtained. The measured values were compared with the calculated values, as shown in Table 3.

From the test results in Table 3, it can be found that the experimental results of the maximum commutation half cycle under the five working conditions measured were smaller than the calculated values by the uncorrected formula, and the relative error exceeded 15%. The reason is that the empirical calculation formula summarized from by

numerical simulation is based on the assumption that there is no heat loss on the wall. In practice, because of the temperature difference between the device wall and the environment, there will be a part of heat loss, resulting in a shorter maximum commutation half cycle. Therefore, the empirical formula based on the numerical simulation needs to be further corrected to be suitable for the practical situation. The wall heat loss correction coefficient  $k$  was introduced to obtain the following complete mathematical model of the maximum commutation half cycle of thermal countercurrent oxidation:

$$T = 23.433kL(1 - \varepsilon)^{1.189}v^{-1.088}e^{0.654}, \quad (9)$$

where  $k$  is the wall heat loss correction coefficient, which is related to the thermal insulation performance of the device, generally set to 0.8-0.9. The thermal insulation performance of the device body of this experimental system is poor. Thus, the wall heat loss coefficient was set to  $k=0.82$  for correction. As shown in Table 3, after correction, the relative error between the calculated value and the measured value does not exceed 3.0%, indicating that the maximum commutation half cycle calculated by the complete mathematical model is consistent with the measured data. Therefore, the obtained formula can be applied to the design calculation of the maximum commutation half cycle for thermal countercurrent oxidation system of low-concentration gas in the actual coal mine ventilation.



TABLE 3: Comparison of experimental and calculated values of the maximum commutation half cycle.

| Working condition number | Methane concentration (%) | Inlet velocity (m/s) | Porosity | Filling length (m) | Measured value (min) | Calculated value before correction (min) | Error before correction (%) | Calculated value after correction (min) | Error after correction (%) |
|--------------------------|---------------------------|----------------------|----------|--------------------|----------------------|--|-----------------------------|---|----------------------------|
| 1                        | 0.30                      | 0.20                 | 0.56     | 1.20               | 23.17                | 27.77                                    | 16.58                       | 22.77                                   | 1.73                       |
| 2                        | 0.60                      | 0.30                 | 0.70     | 1.20               | 14.33                | 17.83                                    | 19.60                       | 14.62                                   | 1.96                       |
| 3                        | 0.40                      | 0.30                 | 0.56     | 0.80               | 11.50                | 14.38                                    | 20.00                       | 11.79                                   | 2.44                       |
| 4                        | 0.50                      | 0.25                 | 0.70     | 0.80               | 10.33                | 12.86                                    | 19.67                       | 10.55                                   | 2.04                       |
| 5                        | 0.70                      | 0.35                 | 0.70     | 1.20               | 13.33                | 16.67                                    | 20.04                       | 13.67                                   | 2.49                       |
| 6                        | 0.30                      | 0.20                 | 0.36     | 1.2                | 36.51                | 43.36                                    | 15.79                       | 35.55                                   | 2.69                       |
| 7                        | 0.60                      | 0.30                 | 0.4      | 1.2                | 34.27                | 40.65                                    | 15.69                       | 33.33                                   | 2.82                       |
| 8                        | 0.40                      | 0.30                 | 0.36     | 0.8                | 18.51                | 22.44                                    | 17.53                       | 18.40                                   | 0.57                       |
| 9                        | 0.50                      | 0.25                 | 0.4      | 0.8                | 23.73                | 29.33                                    | 19.09                       | 24.05                                   | 1.33                       |
| 10                       | 0.70                      | 0.35                 | 0.4      | 1.2                | 31.82                | 38.02                                    | 16.30                       | 31.17                                   | 2.07                       |

## 6. Conclusions

In this study, the orthogonal experiment design method was used to obtain the maximum commutation half cycle for thermal countercurrent oxidation of coal mine ventilation gas under 25 working conditions using the Fluent computational fluid dynamics software. In addition, the relationship between the maximum commutation half cycle and various factors was analysed. From the results of the numerical simulation analysis, it can be seen that the maximum commutation half cycle was closely related to the methane concentration of ventilation gas, the inlet velocity, the porosity of the honeycomb ceramic, and the filling length of the oxidation bed. When other conditions were constant, the maximum commutation half cycle of thermal countercurrent oxidation increased with the increase of intake methane concentration of ventilation gas and filling length, while decreased with the increase of air inlet velocity and porosity of oxidation bed. On this basis, the SPSS data processing software was used to perform regression analysis on the numerical simulation data, and the multiple regression equations with four influencing factors including methane concentration, inlet velocity, porosity, and filling length of oxidation bed were obtained. The deviation between the predicted values and the data simulation values was small, and the degree of fit was high. In addition, the maximum commutation half cycle obtained by the numerical simulation was verified by experiments. After introducing the wall heat loss correction coefficient, the complete mathematical model for the calculation of the maximum commutation half cycle was obtained. The experimental results and the calculated results after correction were compared, and the relative error was not more than 3%. The complete mathematical model after correction can be applied to the design calculation of the maximum commutation half cycle for thermal countercurrent oxidation of low-concentration gas in the actual coal mine ventilation. Because of the limitation of experimental parameters, the prediction model has certain limitations. Therefore, to improve the accuracy of the maximum commutation half cycle prediction, it is necessary to supplement a larger amount of numerical simulations and experiments, as well as more accurate data fitting methods.

## Data Availability

Data sharing is not applicable to this article as no datasets were generated or analysed during the current study.

## Conflicts of Interest

The authors declare that they have no conflicts of interest.

## Acknowledgments

This research was financially supported by the National Natural Science Foundation of China (51774135 and 51974120), Hunan Postgraduate Research and Innovation Funding Project (CX2018B657), and Southern Coal Mine Gas and Roof Disaster Prevention and Control Work Safety Key Laboratory Open Fund Project (E21825).

## References

- [1] J. F. Zhang, S. L. Shi, Y. Lu, and Y. Bo, "Symbiotic disasters of mine gas and coal spontaneous combustion: coupling relationship, disaster mechanism, prevention and control technology," *China Safety Science Journal*, vol. 30, no. 10, pp. 149–155, 2020.
- [2] Y. J. Li, P. F. Wang, R. H. Liu, Y. Jiang, and H. Han, "Determination of the optimal axial-to-radial flow ratio of the wall-mounted swirling ventilation in fully mechanized excavation face," *Powder Technology*, vol. 360, pp. 890–910, 2020.
- [3] Y. J. Li, P. F. Wang, R. H. Liu, and R. Gao, "Optimization of structural parameters and installation position of the wall-mounted air cylinder in the fully mechanized excavation face based on CFD and orthogonal design," *Process Safety and Environmental Protection*, vol. 130, pp. 344–358, 2019.
- [4] S. L. Shi, A. Y. Wu, R. Q. Li et al., "Numerical simulation and scheme optimization on gas drainage through high level borehole in working face," *Journal of Safety Science and Technology*, vol. 12, no. 7, pp. 71–76, 2016.
- [5] S. Y. Hu, Y. Gao, G. R. Feng, F. Hu, C. Liu, and J. Li, "Experimental study of the dust-removal performance of a wet scrubber," *International Journal of Coal Science & Technology*, vol. 8, no. 2, pp. 228–239, 2021.
- [6] P. F. Wang, X. H. Tan, L. Y. Zhang, Y. Li, and R. Liu, "Influence of particle diameter on the wettability of coal dust and

- the dust suppression efficiency via spraying,” *Process Safety and Environmental Protection*, vol. 132, pp. 189–199, 2019.
- [7] Y. H. Niu, “Prospect and utilization status of Low concentration gas in vitiated air at mines,” *Industrial Safety and Environmental Protection*, vol. 28, no. 3, pp. 3–5, 2002.
- [8] X. Y. Wang and J. Du, “Present situation and prospect of oxidation technology about mine methane with concentration less than 1%,” *Coal Technology*, vol. 27, no. 9, pp. 1–3, 2008.
- [9] F. K. Zhang and L. J. Xu, “Effect of methane on global warming and mitigating measure,” *Mining Safety & Environmental Protection*, vol. 31, no. 5, pp. 6–9, 2004.
- [10] B. Zhang, Y. Q. Liu, R. X. Liu et al., “Oxidation of coal mine ventilation air methane in thermal reverse-flow reactor,” *Journal of China Coal Society*, vol. 34, no. 11, pp. 1475–1478, 2009.
- [11] Y. Lu, F. Jiang, and Y. H. Xiao, “Experimental study of coal mine ventilation air methane oxidization,” *Journal of China Coal Society*, vol. 36, no. 6, pp. 973–977, 2011.
- [12] S. Su, A. Beath, H. Guo, and C. Mallett, “An assessment of mine methane mitigation and utilisation technologies,” *Journal of China Coal Society*, vol. 30, no. 23, pp. 123–170, 2005.
- [13] W. Krzysztof, “Harnessing methane emissions from coal mining,” *Process Safety and Environmental Protection*, vol. 86, no. 5, pp. 315–320, 2008.
- [14] P. F. Wang, T. Feng, S. L. Li, and P. Ma, “Resistance characteristics of thermal reverse-flow oxidation bed for coal mine ventilation air methane,” *Natural Gas Industry*, vol. 32, no. 6, pp. 73–77, 2012.
- [15] J. R. Shi, M. Z. Xie, and L. Zhou, “Flammable limits and maximum half cycle for inert porous medium burner with reciprocating flow,” *CIE Journal*, vol. 58, no. 2, pp. 1983–1988, 2007.
- [16] P. F. Wang, T. Feng, and X. L. Hao, “One-dimensional numerical simulation of thermal reverse-flow oxidation of ventilation air methane in coal mine,” *Journal of Mining & Safety Engineering*, vol. 29, no. 3, pp. 434–439, 2012.
- [17] E. B. Liu, D. C. Tian, W. S. Li, J. Chen, and Q. Chen, “Study on erosion behavior and separation efficiency of a shale gas vertical separator,” *Energy & Fuels*, vol. 35, pp. 3878–3886, 2021.
- [18] E. B. Liu, X. J. Wang, and W. W. Zhao, “Analysis and research on pipeline vibration of a natural gas compressor station and vibration reduction measures,” *Energy & Fuels*, vol. 35, pp. 479–492, 2021.
- [19] E. B. Liu, D. J. Li, W. S. Li et al., “Erosion simulation and improvement scheme of separator blowdown system —a case study of Changning national shale gas demonstration area,” *Journal of Natural Gas Science and Engineering*, vol. 88, Article ID 103856, 2021.
- [20] Z. H. Lu, “Calculation of effective thermal conductivity of foam porous media,” *Journal of Nanjing University of Science and Technology*, vol. 25, no. 3, pp. 257–261, 2001.